



Contents lists available at ScienceDirect

Structures

journal homepage: <http://www.elsevier.com/locate/structures>

## Robustness of simple joints in pultruded FRP frames

Jawed Qureshi <sup>a,\*</sup>, J. Toby Mottram <sup>b,1</sup>, Behrouz Zafari <sup>b,2</sup>

<sup>a</sup> School of Architecture, Computing and Engineering (ACE), University of East London, 4–6 University Way, Beckton, London E16 2RD, UK

<sup>b</sup> Civil Research Group, School of Engineering, University of Warwick, Coventry CV4 7AL, UK

### ARTICLE INFO

#### Article history:

Received 14 October 2014

Received in revised form 19 March 2015

Accepted 27 March 2015

Available online xxxx

#### Keywords:

Progressive collapse

Structural robustness

Tying capacity

Web cleated connections

Structural integrity

### ABSTRACT

Structural robustness of simple beam-to-column joints in pultruded frames is assessed through tension pull tests. The tying capacity and failure modes are determined from static tests on two batches of specimens for six joints. Tying resistance is an important joint property for maintaining structural integrity in frames in case of accidental loads. No tests have been previously reported to investigate this key structural property for the design of Pultruded Fibre Reinforced Polymer (PFRP) structures. The tension pull tests consist of a PFRP Wide Flange (WF) section bolted to a stiff steel baseplate by a pair of PFRP web cleats, and at the other end the tensile load is applied. One batch of three specimens has a WF 254 × 254 × 9.53 mm section with 100 × 9.53 mm cleats of equal leg-angle material and the other has a WF 203 × 203 × 9.53 mm with angles of size 75 × 9.53 mm. Tension versus displacement curves are plotted to establish linear-elastic response, damage onset, non-linear response and ultimate tensile strength. Damage initiation is characterised by audible acoustic emissions. The load-displacement curve remains linear elastic up to 0.35 to 0.4 of the maximum (ultimate) tension force and damage happens at 0.6 of the ultimate value. Failure is from excessive delamination cracking emanating in the region of a cleat's fillet radius. A model to predict tying resistance is proposed, and successfully calibrated against experimental results. The most important finding of this study is that a pair of 9.53 mm thick PFRP leg-angle web cleats should possess an adequate tying capacity for design against disproportionate collapse.

© 2015 The Institution of Structural Engineers. Published by Elsevier Ltd. All rights reserved.

### 1. Introduction

Pultruded Fibre Reinforced Polymer (PFRP) shapes that mimic steel sections have been employed in structural engineering applications for over 40 years. Pedestrian bridges, cooling towers, building frames, platforms and stair towers are some of the FRP structures with PFRP members. They are preferred, where corrosion and chemical resistance is required, such as in food processing plants, cooling towers and offshore platforms. Another desirable property of FRPs with glass fibres is their electromagnetic transparency, which makes them ideal for radio masts and radomes. They are suitable for structural engineering applications requiring quick installation and lightweight solutions [1–5].

Pultrusion is the most economical way of producing constant thin-walled shapes of FRP material [6]. Standard PFRP shapes consist of E-glass fibre reinforcement (layers of unidirectional rovings and mat) in a thermoset (typically, polyester or vinyl ester) resin based matrix. Their shapes resemble counterparts found in structural steelwork, and they have direct strengths in the longitudinal direction of 200 to

400 N/mm<sup>2</sup> that are similar to structural grade steel. The strengths in the transverse direction are one third of the longitudinal values [3–5]. Modulus of elasticity along the length (20–30 GPa) is typical 1/10th–1/7th of steel and the in-plane shear modulus lies in the range 3 to 5 GPa. The design of PFRP members for framed structures is generally governed by a stiffness (deformation or stability) criterion, rather than by a material strength [1].

Joints, which tie the members together in buildings, are crucial for achieving robustness. Robustness is the ability of a structure to withstand accidental/extreme loading without being damaged disproportionately to the original cause. This loading could be due to “fire, explosions, impact or the consequences of human error” [7]. It means that a structure designed and constructed to have robustness will not suffer from disproportionate collapse (risking the safety of humans above an acceptable level) should a few members and/or joints ultimately fail. In steel framed buildings, robustness is achieved by designing connections (and joints) properly [8]. Since structures formed from PFRP shapes closely resemble steel frames the same robustness strategy can be considered for PFRP structures.

The partial collapse in May 1968 of the 22-storey Ronan Point Tower, Newham, London, was a fatal catalyst for the structural engineering community to take robustness and safety to a new level. The building was constructed through a panel system building technique with pre-cast concrete units stacked to create load-bearing walls and floors; tying together was minimal and gravity actions effectively held the

\* Corresponding author. Tel.: +44 20 8223 2363; fax: +44 20 8223 2963.

E-mail addresses: [J.Qureshi@uel.ac.uk](mailto:J.Qureshi@uel.ac.uk) (J. Qureshi), [J.T.Mottram@warwick.ac.uk](mailto:J.T.Mottram@warwick.ac.uk) (J.T. Mottram), [B.Zafari@warwick.ac.uk](mailto:B.Zafari@warwick.ac.uk) (B. Zafari).

<sup>1</sup> Tel.: +44 24 76 522 528; fax: +44 24 76 418 922.

<sup>2</sup> Tel.: +44 24 76 573 366; fax: +44 24 76 418 922.

panels in place. A domestic gas explosion occurred in a corner flat at the 18th floor, blowing out two orthogonal walls and causing progressive collapse above and down the full tower height. The failure happened in two stages, initially upwards to the topmost 22nd floor, and next progressively downwards due to the debris falling under gravity [9]. The main reason for the disproportionate failure was lack of a structural frame to tie the precast units together. This seminal 'learning from failure' incident led, throughout the world, to new design provisions for structural robustness in design codes and building regulations. The main emphasis has been on using ductile materials to provide sufficient redundancy within structures so that forces transfer to alternative load paths in case of any accidental load scenario.

Following the partial failure of the Ronan Point Tower, the Building Regulation in the UK now known as Approved Document A [10], was introduced with provisions to avoid disproportionate collapse. These provisions now include:

- (a) A 'tying force' approach, which uses effective horizontal and vertical ties to ensure that a building is robust enough to sustain localised failure;
- (b) 'notional member removal or bridging' provisions, which only need to be considered if tying is not practical. The bridging is achieved by notionally removing an untied element at a time and checking that the region of failure is localised and constrained;
- (c) 'key element' approach should be applied to members where notional removal could cause excessive deformation.

These members should be designed as key elements to withstand a load case with design action of  $34 \text{ kN/m}^2$ . This pressure value comes directly from the estimated average pressure at blow-out on the 18th floor flank panel wall at Ronan Point [11–13].

Annex A of BS EN 1991-1-7 [7] provides a method to categorise buildings in four consequences classes and suggests robustness strategies accordingly. The building classification in EN 1991-1-7 [7] is broadly similar to the one in the UK's Building Regulations Approved Document A [10]. The robustness strategy for specific consequences classes is tabulated in Table 1. Since the majority of, if not all, PFRP structures are going to be less than four storeys high they belong to consequences Class 1 in Table 1, with a very limited risk of failure in the event of accidental loading. No additional robustness strategy is required for building Class 1 as per EN 1991-1-7 [7]; only minimum horizontal tying is recommended. The aim of the tying is to ensure that beam-to-column joints are not damaged in case of relatively small horizontal or vertical loads on the beams. The minimum horizontal tying, in a steel framed building, is provided by ensuring that all steel beam-to-column joints are designed to sustain a tensile force of 75 kN. This requirement is in accordance with

Eurocode 1 Part 1–7 (refer to Table 1). There is no such guideline in Europe or elsewhere for minimum tying resistance for PFRP joints in framed structures.

In North America an ASCE pre-standard for *Load and Resistance Factor Design (LRFD) of pultruded Fibre Reinforced Polymer (FRP) structures* [14] does propose design guidance for a minimum horizontal tying forces. In the mandatory part Section 2.9 [14] states, "Notwithstanding the required connection strength determined from structural analysis, the design strength of structural connections shall not be less than 1 kip (4.5 kN). Should a column lose its continuity, below the locations where beams are connected, and the FRP clip angles are required to take tension action, to prevent disproportionate collapse...". In this paper the meaning of the word 'connection' as used in [14] is 'joint' since Eurocode terminology is preferred. There is no provenance to the rationale for the target tying force being 4.5 kN. The single reference in the pre-standard's commentary giving experimental evidence is the component testing by Turvey and Wang [15] that showed PFRP leg-angles are likely to possess this required strength.

In general, robustness can be provided by tying, bridging and key element design approaches. Because building height shall not exceed 4–5 storeys, the tying force method is the appropriate approach with PFRP structures. It relies on development of catenary action to redistribute actions in the event of a column loss. Byfield and Paramasivam [16] propose that the tension resistance of steel joints should be at least equal to the design shear force in practical applications. The tying force approach has been criticised [12,16] because it ignores the effects of dynamic amplification and the high connection ductility demands in the wake of sudden column loss. Given that PFRP structures would not require any additional robustness measures the tying force provision is the practical robustness strategy to be developed and implemented.

Robustness of simple PFRP joints is an under-researched topic with no specific targeted research conducted to-date. No experimental evidence exists towards understanding the tying capacity of beam and column joints. To the authors' knowledge there is only single paper by Turvey and Wang [15] reporting test results for the tensile response of PFRP angle-leg junctions. In their work the tensile capacity of an isolated equal leg-angle was determined by clamping one leg against a steel plate while the orthogonal leg was pulled until the PFRP failed. The main conclusion from the Turvey and Wang [15] test series was that leg-angles are likely to possess a tensile strength in excess of 4 kN. Because their test configuration does not represent the geometry in beam-to-column (simple) joints [4] it was decided to carry out a test series that more closely represents construction practice.

The main aim of the research reported in this paper is to establish the tying capacity of simple beam-to-column joints with PFRP web cleats. A series of tests comprising two batches of three specimens (with two web cleats per specimen) have been conducted to determine the horizontal tying resistances for two different joint details. The

**Table 1**  
Robustness strategy according to building type and occupancy as per BS EN 1991-1-7 [7] and Approved Document A [10].

| Consequences class  | Building type and occupancy  | Robustness strategy   |
|---|--|---|
| Class 1<br><i>Low consequences of failure</i>                           | Single occupancy houses not exceeding 4 storeys.   | Additional measures not required, but min horizontal tying recommended  |
| Class 2a<br>(Lower risk group)<br><i>Medium consequences of failure</i> | 5 storey single occupancy houses.  | Tying: Minimum horizontal tying i.e. beam-to-column connections to take 75 kN tensile load  |
| Class 2b<br>(High risk group)<br><i>Medium consequences of failure</i>  | Hotels, flats, apartments and other residential buildings greater than 4 storeys but not exceeding 15 storeys. | Tying: Horizontal and vertical Ties<br>Bridging: A structure designed to bridge over a loss of an untied member by notionally removing each untied element, and checking the area at risk of collapse is limited to:<br>a. 15% of the area of the storey or,<br>b. $100 \text{ m}^2$ .<br>Key element: a member should be designed as a key element capable of sustaining additional loads related to a pressure of $34 \text{ kN/m}^2$ .<br>A systematic risk assessment of the building should be undertaken. |
| Class 3<br><i>High consequences of failure</i>                          | All buildings defined above that exceed the limits on area and number of storeys.                              | A systematic risk assessment of the building should be undertaken.  |

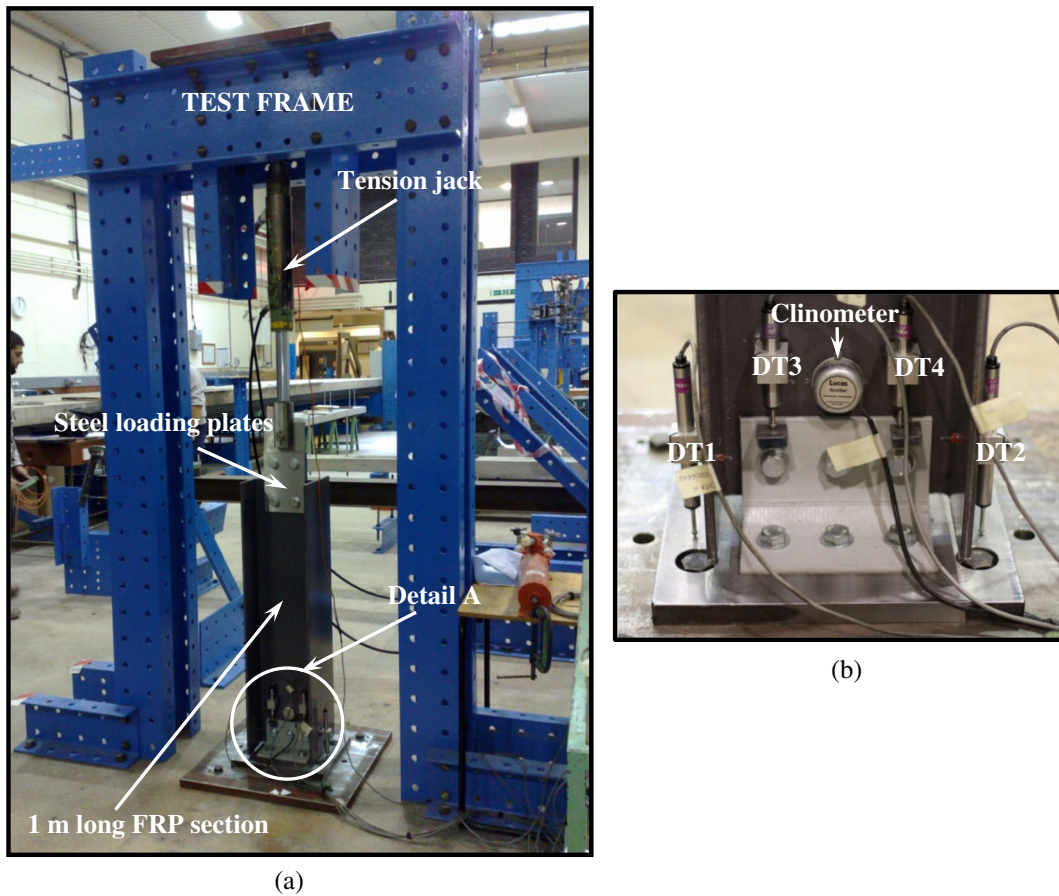


Fig. 1. General test arrangement for tension pull test with a 254 × 254 × 9.53 mm specimen: (a) test arrangement; (b) detail A.

experimentally derived tension strengths are compared with the robustness provision given in the ASCE pre-standard [14]. Presented, and evaluated are the failure patterns and tensile (tying) load against axial displacement plots. Developed to predict the tensile capacity is a new closed-form expression based on geometry and the transverse flexural strength of the cleat (PFRP) material.

2. Test configuration

Fig. 1 has photographs showing the experimental arrangement. Shown in part (a) is the overall details, and in part (b) there is a zoomed-in view for the local joint region. One end of the PFRP beam, in a vertical position, is bolted to a 20 mm thick steel baseplate by

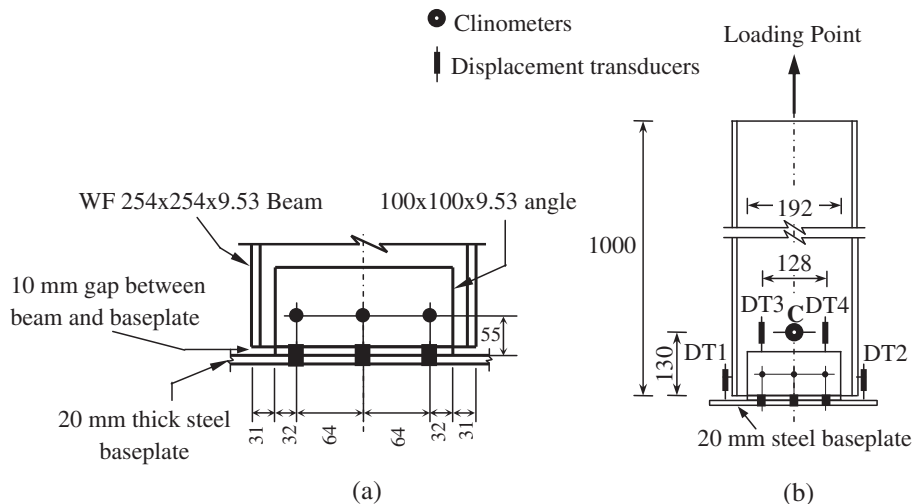


Fig. 2. Connection details and instrumentation for a 254 × 254 × 9.53 mm specimen (all dimensions are in mm): (a) connection details; (b) instrumentation.

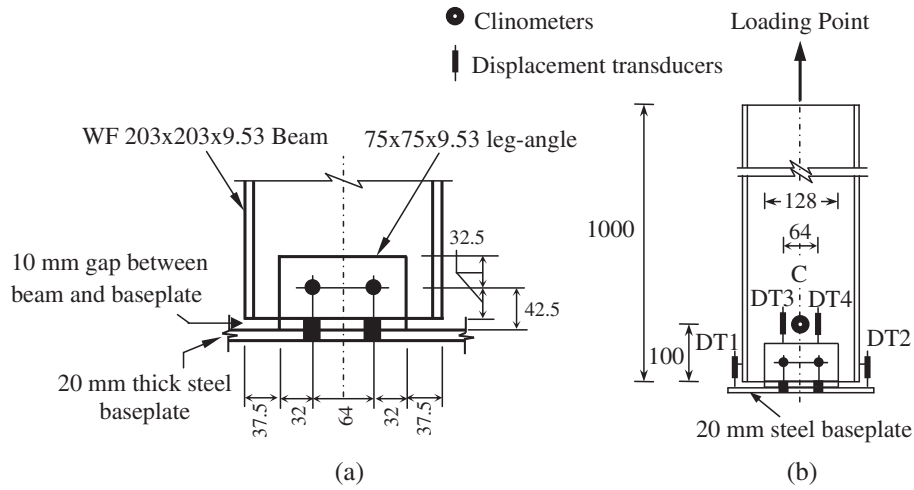


Fig. 3. Connection details and instrumentation for a 203 × 203 × 9.53 mm specimen (all dimensions are in mm): (a) connection details; (b) instrumentation.

means of FRP leg-angles of 9.53 mm thickness. The baseplate itself is bolted to a second steel plate, which is firmly attached to a strong floor by means of M20 steel anchor bolts. This test arrangement gives a rigid base. In practice the column flange outstands will experience flexural deformations. Because damage occurs and grows in a cleat at the fillet radius the difference in stiffness from having a steel base plate is not believed to be of importance. At the other end of the 1000 mm long WF section is the tension hydraulic jack connected via alloy steel plate fixtures.

The testing programme comprises two batches, each having three identical specimens and thereby six web cleats. Batch one has three bolts per cleat leg, and is labelled TP254\_3M16 for Tension Pull test with 254 × 254 × 9.53 mm beam and a single row of 3 M16 bolts. The dimensions for the equal leg-angle are 100 × 100 × 9.53 mm (for size 100 × 9.53 mm). Similarly, batch two has label TP203\_2M16 for a 203 × 203 × 9.53 mm beam, 75 × 75 × 9.53 mm leg-angle (for size 75 × 9.53 mm), and 2 M16 bolts per cleat. WF beams and leg-angles are products in the Pultex® SuperStructural 1525 series from the American pultruder Creative Pultrusions Inc. Mechanical properties for structural engineering works are given in tables in the pultruder's Design Manual [3].

2.1. Static loading procedure

As seen in Fig. 1(a) two steel loading plates are bolted to the beam's web. An inner steel plate is connected to a steel socket by means of an EN24 T high tensile alloy steel pin. The socket is attached to the hydraulic jack to ensure vertical load alignment with the centroid of the joint geometry. Tensile load is applied statically through a manually operated jack and measured using a 45 kN load cell that is attached above the jack. The height of the cross-member in the blue-meccano frame was

adjusted so that, prior to tensile loading, there is 250 mm travel in the jack. Testing was under load control with 2.5 kN increments for the 254 × 254 × 9.53 mm specimens (TP254) and 2 kN increments for the smaller 203 × 203 × 9.53 mm specimens (TP203). Between the two increments of load a time lapse of 2–5 minutes is employed to inspect and record visual observations. Every two seconds test data were continuously stored in real time onto a data logger. Duration of a single strength test was about 1–2 hours.

2.2. Connection details and instrumentation

Figs. 2 and 3 are for engineering drawings to illustrate joint details in accordance with those given in the Strongwell Design Manual [4]; this is a second American pultruder, who with Creative Pultrusions Inc. have been instrumental in supporting the writing of the ASCE LRFD pre-standard [14]. Dimensions for the two simple joints were chosen to satisfy the minimum requirements for bolted connections in [14]. The same connection detailing has been used previously by Qureshi and Mottram [17,18] when determining the moment-rotation behaviour of PFRP beam-to-column simple joints. Steel bolts of grade 8.8 M16 with 35 mm diameter by 3 mm thick steel washers are used in specimen fabrication. As recommended in [14,19] the steel bolting is preloaded to a bolt torque of 40 Nm to represent the snug-fit condition. Further information about the detailing used is given in [17,18].

Figs. 2 and 3 are used to identify the locations for displacement (strain gauge based) transducers and a clinometer. Displacement transducers DT1 and DT2 record the axial displacement with respect to the steel baseplate on left and right sides of the beam. It should be noted that this axial displacement is for a measure of the deformation of web cleats owing to their flexural/shear stiffness and influence of stress concentration around bolt holes and geometry changes from

Table 2 Summary of tension pull test results for batch TP254\_3M16 (compensated for slip).

| Specimen label (1)   | $P_i$ (kN) (2) | $\Delta_i$ (mm) (3) | $S_i = P_i/\Delta_i$ (kN/mm) (4) | $P_j$ (kN) (5) | $\Delta_j$ (mm) (6) | $S_j = P_j/\Delta_j$ (kN/mm) (7) | $P_{max}$ (kN) (8) | $\Delta_{max}$ (mm) (9) |
|----------------------|----------------|---------------------|----------------------------------|----------------|---------------------|----------------------------------|--------------------|-------------------------|
| TP254_3M16_1 (Left)  | 9.0            | 0.55                | 16                               | 14.2           | 1.2                 | 12                               | 24.0               | 4.0                     |
| TP254_3M16_1 (Right) | 9.0            | 0.37                | 24                               | 14.2           | 1.0                 | 14                               | 24.0               | 3.6                     |
| TP254_3M16_2 (Left)  | 8.5            | 0.56                | 15                               | 14.5           | 1.3                 | 11                               | 25.3               | 5.4                     |
| TP254_3M16_2 (Right) | 9.0            | 0.52                | 17                               | 14.5           | 1.2                 | 12                               | 25.3               | 5.2                     |
| TP254_3M16_3 (Left)  | 8.5            | 0.38                | 22                               | 15.4           | 1.3                 | 12                               | 25.0               | 4.4                     |
| TP254_3M16_3 (Right) | 8.7            | 0.33                | 26                               | 15.4           | 1.0                 | 15                               | 25.0               | 4.0                     |
| Mean for six cleats  | 8.8            | 0.45                | 20                               | 14.7           | 1.2                 | 13                               | 24.8               | 4.4                     |
| CV for six cleats    | 2.8%           | 23%                 | 23%                              | 3.7%           | 11%                 | 11%                              | 2.5%               | 16%                     |

**Table 3**

Summary of tension pull test results for batch TP203\_2M16 (compensated for slip).

| Specimen label<br>(1) | $P_i$<br>(kN)<br>(2) | $\Delta_i$<br>(mm)<br>(3) | $S_i = P_i/\Delta_i$<br>(kN/mm)<br>(4) | $P_j$<br>(kN)<br>(5) | $\Delta_j$<br>(mm)<br>(6) | $S_j = P_j/\Delta_j$<br>(kN/mm)<br>(7) | $P_{max}$<br>(kN)<br>(8) | $\Delta_{max}$<br>(mm)<br>(9) |
|-----------------------|----------------------|---------------------------|--|----------------------|---------------------------|--|--------------------------|-------------------------------|
| TP203_2M16_1 (Left)   | 8.0                  | 0.38                      | 21                                     | 12.1                 | 0.70                      | 17                                     | 19.3                     | 3.9                           |
| TP203_2M16_1 (Right)  | 8.2                  | 0.26                      | 31                                     | 12.1                 | 0.57                      | 21                                     | 19.3                     | 3.9                           |
| TP203_2M16_2 (Left)   | 8.2                  | 0.28                      | 29                                     | 11.9                 | 0.60                      | 20                                     | 19.5                     | 3.7                           |
| TP203_2M16_2 (Right)  | 8.3                  | 0.29                      | 28                                     | 11.9                 | 0.60                      | 20                                     | 19.5                     | 3.7                           |
| TP203_2M16_3 (Left)   | 8.3                  | 0.29                      | 29                                     | 12.7                 | 0.76                      | 17                                     | 19.8                     | 4.4                           |
| TP203_2M16_3 (Right)  | 8.7                  | 0.30                      | 29                                     | 12.7                 | 0.66                      | 19                                     | 19.8                     | 4.3                           |
| Mean for six cleats   | 8.3                  | 0.30                      | 28                                     | 12.3                 | 0.65                      | 19                                     | 19.5                     | 4.0                           |
| CV for six cleats     | 2.9%                 | 14%                       | 13%                                    | 2.9%                 | 11%                       | 9%                                     | 1.2%                     | 8%                            |

developing delamination cracking. It is in no way to be associated with either axial displacement of the beam or the leg-angle itself because no discernible axial deformations occurred in these two joint components. Displacement transducers DT1 and DT2 are attached to the beam's flanges. Similarly, displacement transducers DT3 and DT4 measure the relative slip deformation between the web cleat and beam. DT1 and DT2 have a 50 mm stroke range, while DT3 and DT4 gave 25 mm of travel. The clinometer, labelled C, is located in between DT3 and DT4 and records the rotation in the plane of the web. Due to limited space between DT3 and DT4 with the smaller TP203\_2M16 specimens the clinometer C had to be located at the same position on the rear-side of the three specimens. Displacements are recorded to a resolution of  $\pm 0.01$  mm and rotation to 0.02 mrad (linear to  $\pm 1\%$  over a  $10^\circ$  range). The rotation data is not presented in this paper because it was found to be insignificant, i.e. a maximum value of 2 mrad when the

test was terminated. The purpose of measuring the rotation was solely to check if a specimen had verticality throughout the test.

### 3. Results and discussion

Testing was conducted on two batches having three nominally identical specimens and thereby six web cleats. Tables 2 and 3 presents the test results and Figs. 4 and 5 show failure patterns. Plotted in Figs. 6 and 7 are the tensile load against axial displacement curves. When constructing the plots the relative slip between the web cleat and the beam (as recorded by DT3 and DT4 readings) has been deducted from the overall axial displacement measured by DT1 and DT2 respectively.

Tables 2 and 3 give initial, damage and maximum joint properties from the measured load–displacement responses presented in Figs. 6 and 7. Column (1) gives the specimen label with the last character

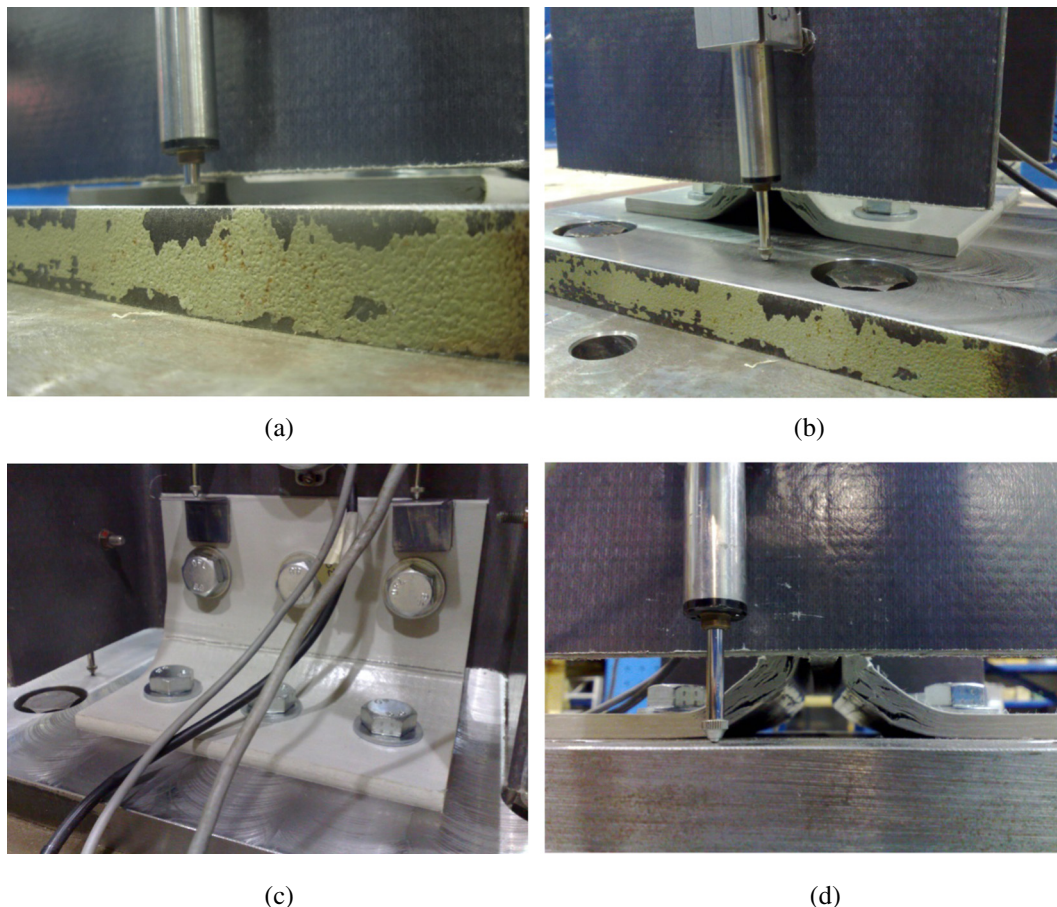


**Fig. 4.** Failure patterns for batch TP254\_3M16: (a) before test; (b) after test; (c) failed web cleat; (d) vertical crack at the point of clamping.

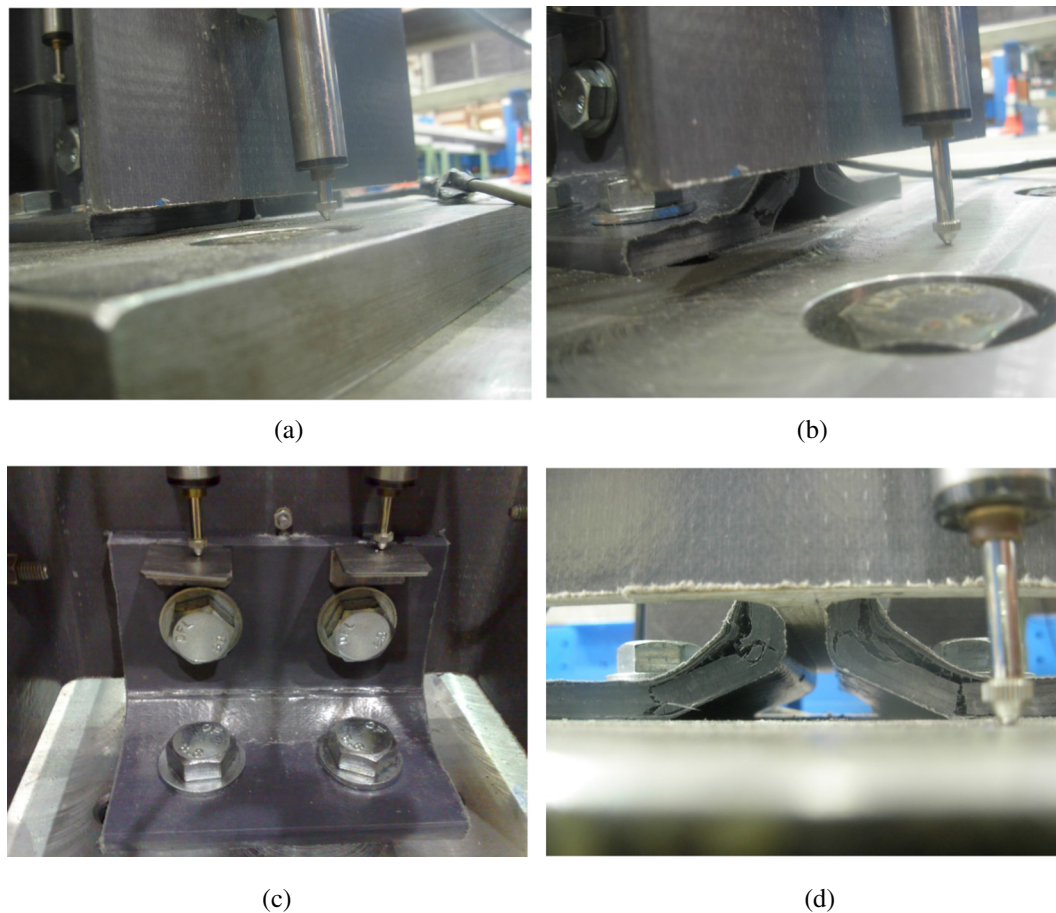


Fig. 5. Failure patterns for batch TP203\_2M16: : (a) before test; (b) after test; (c) failed web cleat; (d) vertical crack at the point of clamping.

giving the specimen number. A label ends by giving 'Left' or 'Right' for the beam's side, which is to conveniently distinguish between the two flange outstands on the column side of the joint. Initial properties in columns (2) to (3) represent the linear elastic response, and are denoted by  $P_i$  for initial load and  $\Delta_i$  for initial axial displacement. The initial stiffness ( $S_i$ ) in column (4) is given by dividing  $P_i$  by  $\Delta_i$ . Similarly  $P_j$ ,  $\Delta_j$  and  $S_j$  in columns (5) to (7) give these three equivalent properties at damage onset, which is defined as the point on the load–displacement curve when audible acoustic emissions are first heard. The authors know from previous joint characterization work [17,18] that this response during testing signals when PFRP delamination failure is occurring, even when hairline cracks within the cleats may not be visible by human inspection. The cleated joints always failed by progressively growing cracks between (for delamination damage) and later through the fibre reinforced layers. A dentist's mirror was used to detect the appearance of the cracks on the side edge surfaces. Due to the constraint from joint geometry (see Figs. 2 and 3) it was a challenge to observe hairline cracks directly by the naked eye. When close to the maximum load, cracking was extensive and was visible. The properties at the maximum tension (for ultimate failure) are reported in columns (8) and (9) of Tables 2 and 3, and are denoted by  $P_{max}$  and  $\Delta_{max}$ . In the bottom two rows of the tables the batch Mean and batch Coefficient of Variation (CV) for the eight properties tabulated are given.

Both TP254 and TP203 batches gave a linear elastic response up to a mean load range of 8–9 kN, with the smaller joint 1.4–1.5 times stiffer ( $S_i$  and  $S_j$ ) than the larger sized joint. Damage onset happened at a mean  $P_j$  of 15 kN for batch TP254 and 12 kN for TP203. At damage onset, a decrease in stiffness of about  $0.35S_i$  is measured. Joints TP254

and TP203 are found to have a mean maximum resistance,  $P_{max}$ , of 25 kN and 19.5 kN. It is found with both joints that the damage load  $P_j$  is close to  $0.60P_{max}$ . From the final row in Tables 2 and 3 it is observed that the CV for the three loads ( $P_i$ ,  $P_j$  and  $P_{max}$ ) is in the range 1–4%, thereby showing a relatively low variation. Because the two axial displacements  $\Delta_i$  and  $\Delta_j$  have a significantly higher variation with CVs from 11 to 23% the calculated axial stiffnesses  $S_i$  and  $S_j$  have higher variation too. The CVs for  $P_j$ ,  $\Delta_j$  and  $S_j$  at onset of failure are similar for both TP254 and TP203 batches.

### 3.1. Failure patterns

The four parts in Figs. 4 and 5 are for photographs showing typical delamination cracking in the web cleats, and adjacent to the fillet radius. Part (a) is before resistance testing commenced, and part (b) afterwards. Part (c) shows a failed web cleat with part (d) used to expose vertical cracks at the line of clamping. This vertical fracturing close to a row of bolts is most prominent in Fig. 5(d), and is where the ultimate failure can be seen to possess a type of hinge mechanism. After disassembly there were no signs of bolt bearing failure in the PFRP beam web [20] or steel bolt failure, and neither of these distinct connection failure modes was expected. Damage within the cleats is assumed to be developing when there are audible acoustic emissions coming from the region of the cleats. Onset is followed by creation of hairline cracking and loss of contact between web cleats and the steel baseplate. Fracturing starts near the fillet radius, and as the tension imposed deformation increased it propagates from the radius along a leg towards the bolt row. Progressive damage growth eventually leads

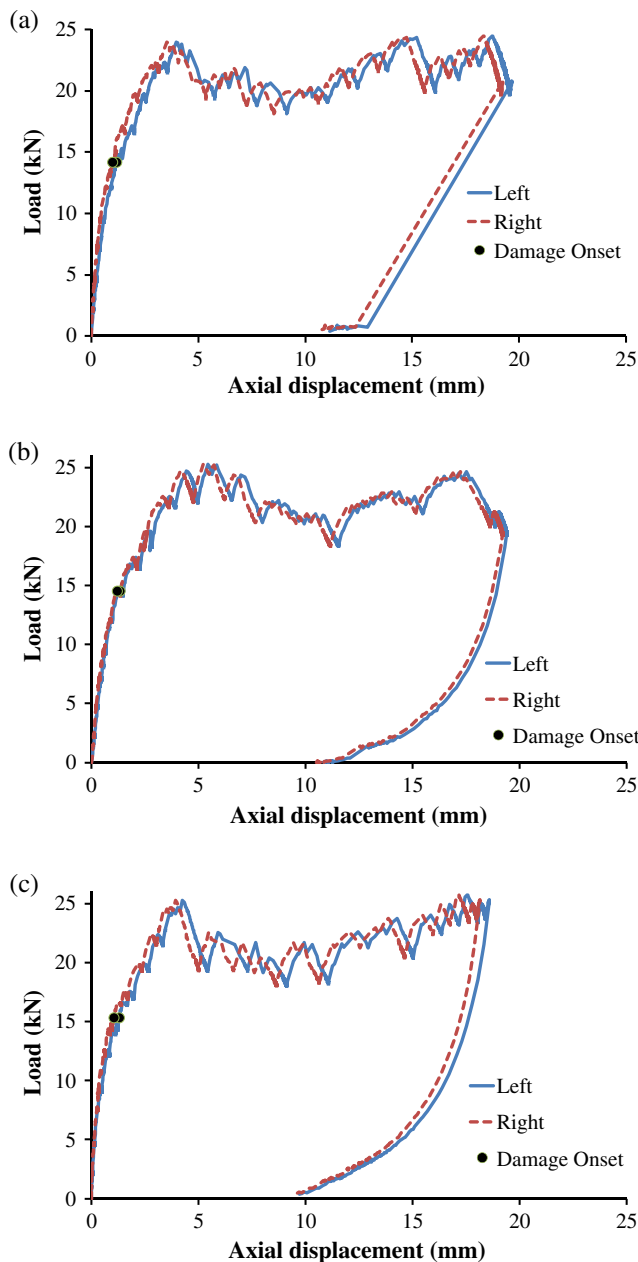


**Fig. 6.** Tensile load against axial displacement curves for batch TP254\_3M16: (a) specimen 1; (b) specimen 2; (c) specimen 3.

to the vertical cracking causing either loss of load-carrying capacity or instability of the specimen. In the case of the TP254 batch the loading was stopped at a displacement of about 18 mm (Fig. 6) because no further increase for  $P_{max}$  (mean of 25 kN) could be expected due to severe delamination cracks.

Fig. 5(d) shows cleat damage in a TP203 specimen. Note that the interface bond between the outer two layers has failed over a reasonable length. Delamination fracturing between the alternating layers of unidirectional rovings and mat are also to be seen in the photograph. The vertical crack (adjacent to the line of clamping) is an indication that ultimate failure has been reached. The appearance of a hinge-type mechanism is a clear sign of imminent failure and a sudden drop in  $P$  at a displacement of 3.7 to 4.3 mm is seen in Fig. 7(a) to (b). Further applied deformation after  $P_{max}$  (mean of 19.5 kN) led to a loss in instantaneous resistance with a rapid decrease in axial stiffness.

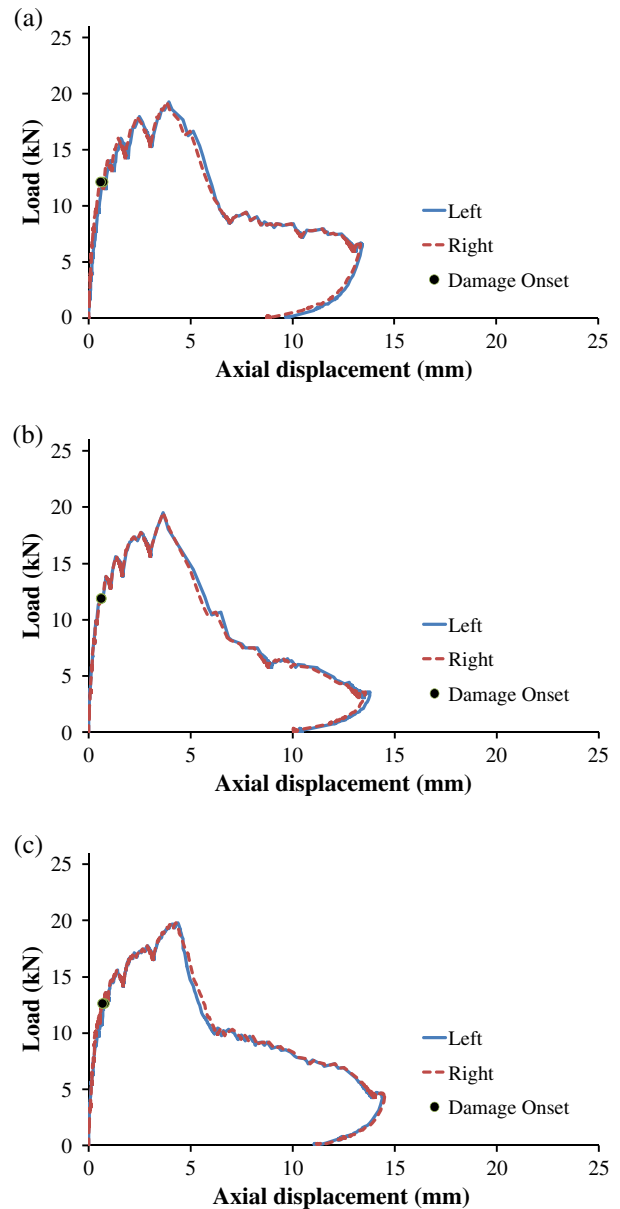


**Fig. 7.** Tensile load against axial displacement curves for batch TP203\_2M16: (a) specimen 1; (b) specimen 2; (c) specimen 3.

### 3.2. Load versus axial displacement behaviour

Plotted in Figs. 6 and 7 are the load against displacement responses. Each figure has three pairs of curves in parts (a) to (c) for Specimens 1 to 3 in batches TP254 and TP203, respectively. A plot has two curves, with the blue solid line for the 'Left' side cleat (DT1 in Figs. 2 and 3) and the red dashed line for the 'Right' (DT2 in Figs. 2 and 3). The black solid circle symbol on the curves in Figs. 6 and 7 is for the load–displacement ( $P_j-\Delta_j$ ) for onset of damage.

For batch TP254 the curves in Fig. 6 show three distinct sections; namely linear elastic, non-linear and post-maximum behaviour. Each of the six curves is seen to remain approximately linear elastic until damage onset ( $P_j$ ) is observed at about 15 kN. Further load increments result in widening of the cracks and the maximum load ( $P_{max}$ ) is attained at about 25 kN, with a corresponding axial displacement of 4.5 mm. A load–displacement curve is found to follow a non-linear response from damage to the maximum load level. The saw-tooth shape of a curve in Fig. 6 indicates stiffness degradation from stiffness

relaxation during the constant ‘stroke’ stage (2–5 min) in a load increment stage. Due to severe damage at the heel of the cleats there is a load drop of  $0.1P_{max}$  to be witnessed at, and beyond the axial displacement for  $P_{max}$ . On further deformation a specimen regains load back up to the  $P_{max}$  level, and there is no significant reduction in the maximum load to a displacement of 18 mm. It is seen from the curves in Fig. 6(a) to (c) that the post-maximum region constitutes a cycling between two load levels for axial displacement from 4.5 mm to 18 mm.

Batch TP203 exhibited the overall load–displacement response shown in Fig. 7(a) to (c). It consists of two sections, for linear elastic and non-linear behaviours. Response remains linear elastic until damage onset at a mean  $P_j$  of 12 kN. Afterwards, hairline cracks become visible to the human eye close to a fillet radius and at  $P_{max}$  of 19.5 kN there is a severe level of PFRP failure. The load–displacement curves in Fig. 7(a) to (c) show non-linearity as a specimen’s stiffness continuously reduces for tension force increasing from  $P_j$  to  $P_{max}$ . Further load increments, beyond the maximum load level, led to an increase in axial displacement with no increase in  $P$ . This indicates that ultimate failure was impending and so the test was terminated.

3.3. Comparison with existing design guidelines

Figs. 8 and 9 are for bar charts to present  $P_j$  for batches TP254 and TP203. The characteristic  $P_j$  determined in accordance with Annex D of Eurocode 0 [21], and the minimum required design tying strength in the ASCE pre-standard [14] are also given in these figures. A characteristic value is given by a solid (horizontal) line, and is from  $(Mean - 1.77 \times SD)$ , assuming the CV is known [21]. This measure of resistance is estimated to be 13.7 kN and 11.6 kN for TP254 and TP203. The ASCE pre-standard tensile force of 4.5 kN is shown by a dashed (horizontal) line. In the absence of any European or other guidelines for the minimum tying resistance to prevent disproportionate collapse in PFRP framed structures a comparison can only be made with what is proposed in the ASCE pre-standard [14]. The test results reported in Figs. 8 and 9 show that the two batches have characteristic values several times  $> 4.5$  kN. The mean maximum tensile capacities of 24.8 kN for TP254 and 19.5 kN for TP203 are found to be 5.5 and 4.3 times higher than the minimum ASCE pre-standard strength. A significant finding from this series of tensile pull tests is that a pair of 9.53 mm thick PFRP leg-angle web cleats should possess adequate tying capacity for design against disproportionate collapse.

3.4. Model for prediction of tying capacity

Fig. 10 is for a line drawing of a cleat to illustrate the typical ultimate failure mechanism observed. The critically fractured regions are close to the fillet radius between the two legs and at the two lines of clamping (adjacent to bolt rows). It is these three regions that experience most

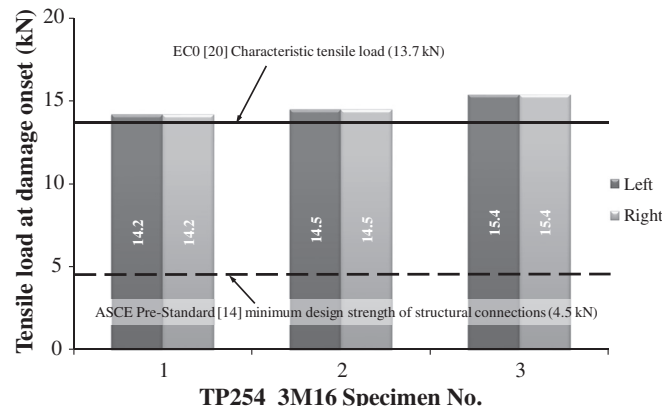


Fig. 8. Characteristic tensile loads for batch TP254\_3M16.

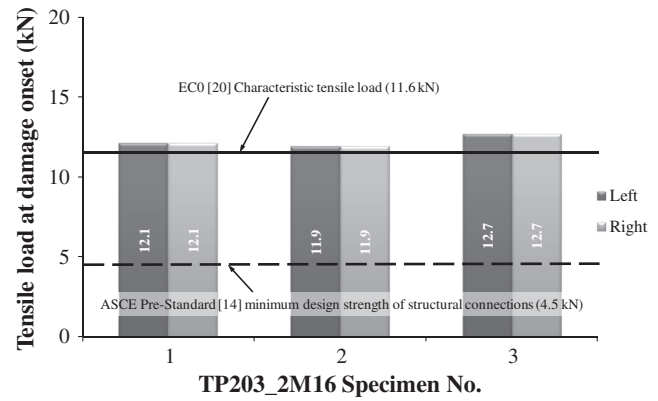


Fig. 9. Characteristic tensile loads for batch TP203\_2M16.

of the through-thickness fracturing due to resisting the flexural/shear deformation from the applied tying force. It is evident from cleat failure seen in Figs. 4 and 5 that a leg-angle ultimately fails due to a combination of extensive delamination damage and a through-thickness fracturing at three ‘hinge’ lines.

Section 15.10, in reference [1], is for simple strength formulae for stresses in out-of-plane shear connections. Section 15.10.2 is for the case of flexural stress in the leg of the angle bolted to the column member and this corresponds to the tying force problem being investigated. Parameters for a PFRP cleat that can influence the magnitude of the tying force,  $T_y$ , are width,  $b$ , thickness,  $t$ , Transverse flexural strength,  $\sigma_{fl,T}$ , and interlaminar shear stress,  $\tau_{TT}$ . Fig. 10 is used to define distance  $B_c$  for the horizontal distance between bolt centreline (on the column side) and the end of connected cleat leg (to the beam web) that also has an important influence. Substituting for these parameters into Eqs. (15.12) and (15.13) from Section 15.10.2 of [1] we have the following two tying capacity expressions:

$$T_y = \frac{8}{3} \times \frac{\sigma_{fl,T} \times b \times t^2}{B_c} \tag{1}$$

and

$$T_y = 2 \times \tau_{TT} \times b \times t. \tag{2}$$

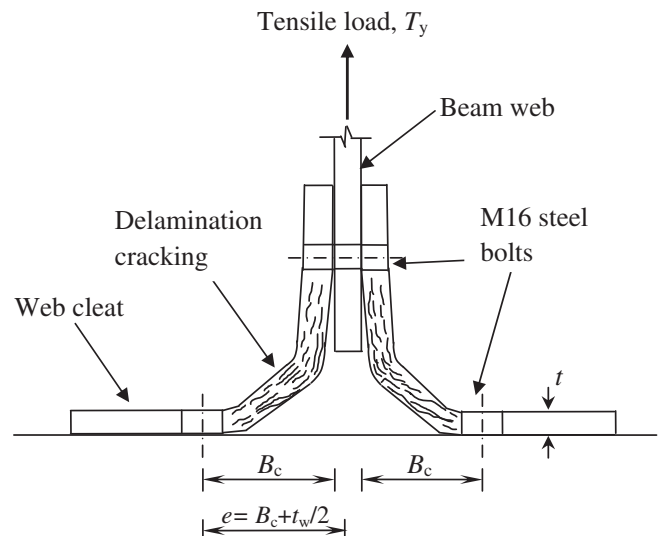


Fig. 10. Schematic line drawing of a failed web cleated joint under tensile load.

Eq. (1) is established assuming linear elastic response with pure bending across the full width of the cleat and  $T_y$  is established when the surface direct stress first reaches  $\sigma_{fl,T}$ . The second formula for  $T_y$  is for interlaminar shear failure on a vertical surface (of area  $b \times t$ ) adjacent to the bolt row holding down the horizontal leg of the angle. The dimensions of the leg-angles are given in Figs. 2 and 3 with  $t$  constant at 9.53 mm, and for TP203  $b$  is 128 mm and  $B_c$  is 42.5 mm, and for TP254  $b$  is 192 mm and  $B_c$  is 55 mm. Mechanical properties of structural shapes are tabulated in Chapter 3 of the pultruder's Design Manual [3]. On pages 12 and 13 are the reported properties for Pultex® SuperStructural 1525 series leg-angle, and from this table  $\sigma_{fl,T} = 165$  MPa and  $\tau_{TT} = 23.4$  MPa.

Reported in Table 4 are the  $T_y$  predictions using Eqs. (1) and (2) with the parameter values just defined. Column (1) gives the labelling for the cleat size and in column (2) the mean experimental tying force (i.e. mean  $P_{max}$ ) presented in Tables 2 and 3. Inspection informs us that the predictions for  $T_y$  in columns (3) and (4) are unreliable using the formulae in Section 15.10 of Bank's book [1] that are based on feasible distinct modes of failure. Because measured tying strengths are < 40% of the lower predictions by Eq. (2) it has to be concluded that the mechanism of failure must involve a complex interaction of through-thickness stresses with concentrations close to the three 'hinge' lines seen in Figs. 4 and 5 and illustrated in Fig. 10.

The authors decided to propose a third closed form expression based on an assumed 'plastic' failure mode in the leg-angle. When the vertical leg in a cleat (connected to the beam web), is subjected to tension it causes the orthogonal leg (connected to the 'column') to deform. Let's assume in the model that the horizontal leg-angle effectively deforms as an end-loaded cantilever beam. The fixed end is at the 'bolt row hinge' line and the end-load is the prying force of  $T_y/2$  taken by the vertical leg. A tying resistance may be established by equating the plastic section moment of resistance to the applied moment. The moment of resistance can be assumed to be  $\sigma_{fl,T} \times b \times t^2/4$  by having the plastic section modulus for the rectangular section of size  $b$  by  $t$ . Parameter  $\sigma_{fl,T}$  is the Transverse flexural strength of the PFRP material. Using the end-loaded cantilever model the moment to be resisted is  $T_y \times e/2$ . Equating the two moments an expression for the tying resistance is

$$T_y = \frac{\sigma_{fl,T} \times b \times t^2}{2e} \tag{3}$$

In Eq. (3)  $e$  is the lever arm, equal to  $B_c$  plus  $0.5t_w$  (half the thickness of the beam web). The approach to formulate the expression is pragmatic because an increase in distance  $e$  (or  $B_c$ ) will increase the prying moment to be resisted, and as a consequence will decrease the tying force in the joint. Predicted  $T_y$ s using Eq. (3) are presented in column (5) of Table 4 and for joints TP254 and TP203 we find that  $T_y$  is 24.6 kN and 20.3 kN, respectively. Their differences with the equivalent mean  $P_{max}$  in column (2) of Table 4 are found to be less than 3%, and because this is a very close agreement for two cleat sizes the model used to formulate Eq. (3) shows promise.

To study the potential of Eq. (3) further, the experimental tying forces in [15] are compared in Table 5 with  $T_{ys}$  by Eq. (3), using the parameter values presented in [15]. Because Turvey and Wang [15] used a single leg-angle the moment to be resisted is  $T_y \times e$ , and so Eq. (3) had to be modified to include a denominator of  $4e$  (to replace  $2e$ ). In their study, one leg was clamped and the other pulled. Assuming that the

**Table 4**  
Experimental ( $P_{max}$ ) and predicted values for tying force  $T_y$ .

| Size (1) | Mean $P_{max}$ (kN) (2) | $T_y$ by Eq. (1) (kN) (3) | $T_y$ by Eq.(2) (kN) (4) | $T_y$ by Eq. (3) (kN) (5) |
|----------|-------------------------|---------------------------|--------------------------|---------------------------|
| TP254    | 24.8 (Table 2)          | 139                       | 86.5                     | 24.6                      |
| TP203    | 19.5 (Table 3)          | 120                       | 50.1                     | 20.3                      |

**Table 5**  
Comparison of experimental tying force from [15] with predicted tying force  $T_y$ .

| Size (1)                        | Specimen label (2) | Actual $b$ (mm) (3) | Exp. tying force (kN) (4) | $T_y$ by Eq. (3) (kN) (5) |
|---------------------------------|--------------------|---------------------|---------------------------|---------------------------|
| 40 mm long<br>75 × 9.5 mm angle | a1                 | 40.6                | 14.3                      | 12.1                      |
|                                 | a2                 | 40.2                | 13.0                      | 11.9                      |
|                                 | a3                 | 40.5                | 13.0                      | 12.0                      |
|                                 | b1                 | 40.2                | 13.3                      | 12.0                      |
|                                 | b2                 | 39.6                | 11.7                      | 11.8                      |
|                                 | b3                 | 40.7                | 13.0                      | 12.1                      |
| Mean                            |                    | 40.3                | 13.0                      | 12.0                      |
| 60 mm long<br>75 × 9.5 mm angle | a1                 | 60.4                | 18.2                      | 18.0                      |
|                                 | a2                 | 60.3                | 18.0                      | 17.9                      |
|                                 | a3                 | 60.4                | 18.4                      | 18.0                      |
|                                 | b1                 | 59.9                | 18.6                      | 17.8                      |
|                                 | b2                 | 60.1                | 17.8                      | 17.9                      |
|                                 | b3                 | 60.6                | 17.4                      | 18.0                      |
| Mean                            |                    | 60.3                | 18.1                      | 17.9                      |

clamping line is 0.5 mm away from the edge of the angle,  $e$  can be taken to be 5.27 mm. Turvey and Wang test series used Strongwell's EXTERN 500 Series equal-leg angles, for which  $\sigma_{fl,T} = 68.9$  N/mm<sup>2</sup> as indicated in Table 1 of the pultruder's Design Manual [4].

Columns (1) to (4) in Table 5 are for Wang and Turvey's contribution presenting from left to right the specimen sizes, the six specimen labels (a1 to a3 and b1 to b3), parameter  $b$  in mm and their experimentally determined tying forces. Column (5) reports the predictions of  $T_y$  using Eq. (3) with parameters defined. Batch means are presented in the table below the tabulated results for a batch of six specimens having  $b$  nominally at 40 or 60 mm. When  $b$  is 40 mm the test mean at 13 kN is 1 kN (8%) higher than the predicted mean. The difference is tying strength reduces to an insignificant 1% (18.1–17.9 = 0.2 kN) when  $b$  is 60 mm. One reason for this improvement in the comparison between theory and practice is that as  $b$  increases the influence of shearing will reduce.

Based on the two favourable comparisons made in this paper the authors are showing that Eq. (3) provides an acceptable prediction for the tying resistance of beam-to-column joints connected together by a pair of PFRP web cleats. Eq. (3) can now be employed, qualitatively, to estimate  $T_y$  for leg-angle sections having different thicknesses. Common thicknesses ( $t$ ) for PFRP leg-angle sections are 6.4 mm, 9.5 mm, 12.7 mm and 15.9 mm, in the range ¼ in. to 5/8 in. [3–5]. Keeping parameters  $b$ ,  $\sigma_{fl,T}$  and  $e$  as specified from the PFRP leg-angle material from Creative Pultrusions Inc., and taking the thinnest and smallest leg-angle cleat to be 75 × 6.4 mm, it is estimated that  $T_y$  is 9.2 kN. Because this predicted  $T_y$  is two times > 4.5 kN it can be proposed that PFRP web angles for simple joints (such as illustrated in Figs. 2 and 3) will possess the required minimum tying resistance as proposed in the ASCE pre-standard [14].

**4. Concluding remarks**

A series of full-sized static tests have been conducted to establish the tying capacity and failure modes for simple beam-to-column joints of pultruded FRP. A new model is proposed to predict the capacity of joints having a pair of bolted web cleats. Testing is split into the two batches for the 254 × 254 × 9.53 mm Wide Flange (WF) section with equal leg-angle cleats of 100 × 9.53 mm and for 203 × 203 × 9.53 mm WF section with cleats of size 75 × 9.53 mm. The following observations are made from the research:

- The most important finding is that a pair of 9.53 mm thick PFRP web cleats will possess the required minimum tying resistance of 4.5 kN in accordance with proposed guidance in Section 2.9 of an ASCE pre-standard [14].
- Tying force versus axial displacement plots remained linear up to 0.35–0.4 of the maximum load; damage onset is found to occur at 0.6 of the ultimate load.

- Failure happens from the onset of non-linearity in the load–displacement response and there is progressive damage development in the web cleats to ultimate failure.
- Damage onset is signalled by audible acoustic emissions and hairline (delamination) cracks only become visible (on the cleat side surfaces) to the human eye when tension force is 0.8 of its ultimate value.
- Predictions from a new simple closed form expression for tying resistance (strength) are found to be within 1–3% of experimental mean results.
- The very close agreement between model resistance and mean measurements from two batches shows that the tying strength for simple pultruded FRP joints having a pair of web cleats is dependent on joint geometry and the flexural strength in the transverse direction.

### Acknowledgements

Authors thank EPSRC (Connections and Joints for Buildings and Bridges of Fibre Reinforced Polymer (EP/H042628/1)) and Access Engineering and Design, Telford, UK, for project funding and supply of FRP material. Skilled assistance from technical staff (Mr Colin Banks (civil engineering), Mr Rob Bromley (workshop) and Mr Graham Canham (photographer)), in the School of Engineering, Warwick University is acknowledged as being invaluable to the quality and future impact of the reported research.

### References

- [1] Bank LC. Composites for construction – structural design with FRP materials. New Jersey: John Wiley & Sons; 2006.
- [2] Bakis CE, Bank LC, Brown VL, Cosenza E, Davalos JF, Lesko JJ, et al. Fiber-reinforced polymer composites for construction state-of-the-art review. *J Compos Constr* 2002;6:73–87.
- [3] Anonymous. The new and improved Pultex® pultrusion design manual. Alum Bank, PA: Creative Pultrusions Inc.; March 06, 2015[[www.creativepultrusions.com/library.html](http://www.creativepultrusions.com/library.html)].
- [4] Anonymous. Strongwell design manual. Bristol, VA: Strongwell; March 06, 2015 [[www.strongwell.com/](http://www.strongwell.com/)].
- [5] Anonymous. Fiberline design manual for structural profiles in composite materials. Kolding, Denmark: Fiberline Composites A/S; March 06, 2015[[www.fiberline.com/read-more-about-fiberline-online-tools](http://www.fiberline.com/read-more-about-fiberline-online-tools)].
- [6] Meyer RW. Handbook of pultrusion technology. London: Chapman and Hall; 1985.
- [7] BS EN 1991-1-7:2006. Eurocode 1 – actions on structures, Part 1–7: general actions – accidental actions. United Kingdom: British Standards Institution; 2006.
- [8] Way AGJ. Structural robustness of steel framed buildings – in accordance with Eurocodes and UK National Annexes, SCI P391, SCI, Ascot; 2011.
- [9] Report of the inquiry into the 'collapse of flats at Ronan Point, Canning Town'. HMSO; 1968.
- [10] Approved document A. The building regulations 2010. Structure. Approved document A (2004 edition incorporating 2004, 2010 and 2013 amendments). HM Government; 2013.
- [11] Byfield M, Mudalige W, Morison C, Stoddart E. A review of progressive collapse research and regulations. *Struct Build* 2014;167(8):447–56.
- [12] Izzuddin BA, Vlassis AG, Elghazouli AY, Nethercot DA. Assessment of progressive collapse in multi-storey buildings. *Proc Inst Civ Eng Struct Build* 2007;160(4):197–205.
- [13] Owens GW, Moore DB. Steelwork connections: the robustness of simple connections. *Struct Eng* 1992;170(3):37–46.
- [14] Pre-standard for load and resistance factor design (LRFD) of pultruded fiber reinforced polymer (FRP) structures (final). American Composites Manufacturers Association, American Society of Civil Engineers; November 9, 2010.
- [15] Turvey GJ, Wang P. Failure of pultruded GRP angle–leg junctions in tension. *Proc. 17th international conference on composite materials (ICCM17)*, 27–31 July 2009, paper A1:1; 2009. p. 11.
- [16] Byfield M, Paramasivam S. Catenary action in steel-framed buildings. *Proc Inst Civ Eng Struct Build* 2007;160(5):247–57.
- [17] Qureshi J, Mottram JT. Moment-rotation response of nominally pinned beam-to-column joints for frames of pultruded fibre reinforced polymer. *Constr Build Mater* 2015;77(2):396–403.
- [18] Qureshi J, Mottram JT. Response of beam-to-column web cleated joints for FRP pultruded members. *J Compos Constr* 2014;18(2):11.
- [19] Gorenc BE, Tinyou R, Syam AA. Steel designers' handbook. Sydney, NSW 2052, Australia: University of New South Wales Press Ltd.; 2005 203–4.
- [20] Mottram JT, Zafari B. Pin-bearing strengths for design of bolted connections in pultruded structures. *Struct Build* 2011;164(5):291–305.
- [21] BS EN 1990:2002. Eurocode 0 – basis of structural design. United Kingdom: British Standards Institution; 2002.